MOLECULAR AND CELLULAR BIOLOGY, Jan. 2004, p. 719–729 Vol. 24, No. 2
0270-7306/04/$08.00+0 DOI: 10.1128/MCB.24.2.719–729.2004

Immunological Function in Mice Lacking the Rac-Related GTPase RhoG

Elena Vigorito,[1]* Sarah Bell,[1] Barbara J. Hebeis,[1] Helen Reynolds,[1] Simon McAdam,[1] Piers C. Emson,[2] Andrew McKenzie,[3] and Martin Turner[1]

Laboratory of Lymphocyte Signaling and Development, Molecular Immunology Programme,[1] and Laboratory of Molecular Neuroscience,[2] The Babraham Institute, Babraham, Cambridge CB2 4AT, and Laboratory for Molecular Biology, Hills Road, Cambridge CB2 2QM,[3] United Kingdom

Received 25 March 2003/Returned for modification 22 April 2003/Accepted 20 October 2003

RhoG is a low-molecular-weight GTPase highly expressed in lymphocytes that activates gene transcription and promotes cytoskeletal reorganization in vitro. To study the in vivo function of RhoG, we generated mice homozygous for a targeted disruption of the *RhoG* gene. Despite the absence of RhoG, the development of B and T lymphocytes was unaffected. However, there was an increase in the level of serum immunoglobulin G1 (IgG1) and IgG2b as well as a mild increase of the humoral immune response to thymus-dependent antigens. In addition, B- and T-cell proliferation in response to antigen receptor cross-linking was slightly increased. Although RhoG deficiency produces a mild phenotype, our experiments suggest that RhoG may contribute to the negative regulation of immune responses. The lack of a strong phenotype could indicate a functional redundancy of RhoG with other Rac proteins in lymphocytes.

Lymphocyte selection and activation requires the integration of the cell cycle, gene transcription, changes in the actin cytoskeleton, and cell adhesion and motility. Monomeric GTPases of the Ras and Rho families have been shown to regulate the survival, proliferation, and differentiation of multiple cell types including lymphocytes (2, 15). At the biochemical level, Rho GTPases function as molecular switches, shuttling between an inactive GDP-bound state and an active GTP-bound state. GTP-bound Rho family proteins bind to and control the activity of a great number of effector proteins (2, 32). Rho GTPases are regulated by three classes of proteins: guanine nucleotide exchange factors (GEFs) promote the transition from the GDP-bound state to the active GTP-bound conformation; GTPase-activating proteins stimulate the inactivation; and guanine nucleotide dissociation inhibitors lock the GTPases in either their active or inactive state.

Transgenic approaches have provided a number of insights into the role of Rho family proteins in lymphocyte development and function. Constitutively activated forms of Rac1 (12), Rac2 (18) and Cdc42 (19) have been overexpressed as transgenes in the mouse thymus and result in a high degree of thymocyte apoptosis. Furthermore, it was demonstrated that active Rac1 could drive T-cell development through the developmental checkpoint that, in normal mice, is dependent upon functional rearrangement of the T-cell receptor (TCR) β-chain gene (β-selection) (12). Moreover, this active Rac1 allele was able to complement deficiency in the Vav-1 GEF (12). By contrast, an active allele of RhoA was unable to mediate this rescue, suggesting that it is the GEF activity of Vav-1 towards Rac family members that is critical for β-selection (5). In addition to this observation, through the use of a specific effector domain mutant of active Rac1 that cannot bind PAK, a role for a Vav-1-Rac-PAK pathway in dominant-negative expansion was excluded (12). The function of the Rho family proteins in T-lymphocyte development has been extensively studied in mice that overexpress clostridium botulinum C3 toxin, which selectively inactivates most members of the Rho family but has little effect on Rac and Cdc42. These studies have demonstrated a role for Rho in both the differentiation and survival of early T-lineage cells (10, 16). More recent studies have defined a role for Rho in the inhibition of p53-dependent apoptosis in early T cells and in the survival and reactivity of T cells at later stages of development (5, 6). In particular, T cells expressing a dominant active version of RhoA were shown to proliferate substantially better than their wild-type counterparts following antigen receptor cross-linking (5).

An alternative approach to facilitate the understanding of GTPase function in lymphocyte development and activation is the generation of knockout mice. In this regard, a lack of Cdc42 (4) and Rac1 (28) has yielded an embryonic lethal phenotype and thus been uninformative with regard to lymphocyte function. The study of Rac2-deficient mice however has revealed the nonredundant role of this GTPase in the function of multiple hematopoietic cell types including neutrophils (25) and mast cells (36) as well as T (17) and B (7) lymphocytes. T lymphocytes deficient in Rac2 are impaired in their ability to polarize their cytokine transcription profile towards the Th1 lineage. In the case of B cells, Rac2-deficient mice display a reduction of B1a and marginal zone B cells as well as reduced humoral immune responses. Moreover, in both thymocytes and B cells, Rac2 has been suggested to be required for optimal calcium release following antigen receptor engagement (7, 17).

The Rho family member RhoG was identified as a serum-inducible gene in fibroblasts and is most similar in structure to

* Corresponding author. Mailing address: Laboratory of Lymphocyte Signaling and Development, Molecular Immunology Programme, The Babraham Institute, Babraham, Cambridge CB2 4AT, United Kingdom. Phone: 44 1223 496 545. Fax: 44 1223 496 023. E-mail: elena.vigorito@bbsrc.ac.uk.

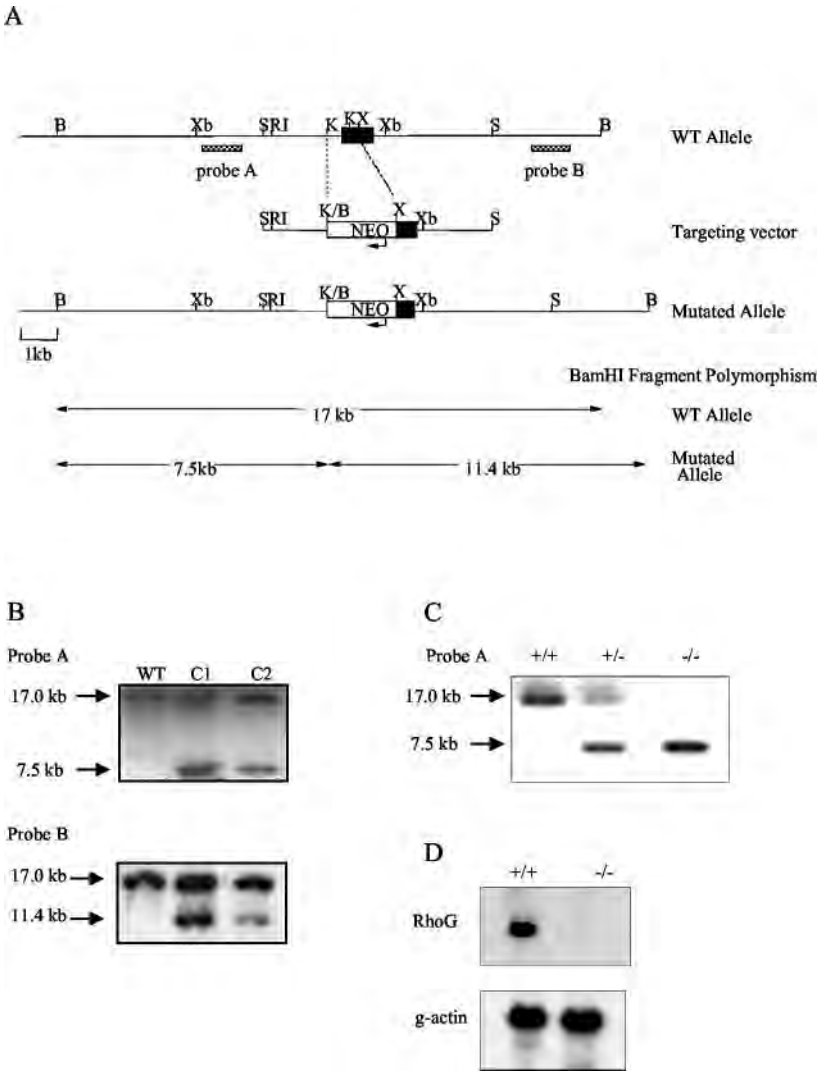

FIG. 1. Targeted disruption of the murine *RhoG* gene by homologous recombination. (A) Schematic representation of the *RhoG* genomic locus, the targeting construct, and the mutated allele. The position of exon 2 is represented by a solid box. The arrows indicate the direction of transcription of the Neo^r gene. The external probes A and B were used for Southern blot analysis from *Bam*HI-digested DNA. The predicted sizes of the fragments generated by *Bam*HI digestion in the wild-type and targeted alleles are indicated in the lower part. B, *Bam*HI; Xb, *Xba*I; S, *Sac*I; RI, *Eco*RI; K, *Kpn*I; X, *Xho*I. (B) Southern blot analysis of the *RhoG* mutation in embryonic stem (ES) cell clones using probes A and B. DNA from wild-type 129/Sv (WT) and ES cell clones (C1 and C2) was analyzed by Southern blotting with probes A and B. The arrows indicate the size of the DNA fragments observed. (C) Tail DNA isolated from wild-type (+/+), *RhoG*$^{+/-}$ (+/−) and *RhoG*$^{-/-}$ (−/−) mice was analyzed using probe A as described above. (D) *RhoG* mRNA expression was analyzed from splenocytes of wild-type and RhoG$^{-/-}$ mice by Northern blotting with a *RhoG* cDNA probe which contains the entire *RhoG* coding sequence. RNA loading was controlled by assessing the levels of γ-actin mRNA.

Rac1, Rac2, and Rac3 (34). Functional studies indicate that an active form of RhoG can cooperate with Ras and Rac to mediate cellular transformation (26). RhoG can activate the c-Jun N-terminal kinase but not the extracellular signal-regulated kinase pathway (26) and induce morphological and cytoskeletal changes in fibroblastoid cells (11). Recent work from our laboratory has shown that RhoG regulated gene transcription in both B and T cells (33). RhoG also promoted cytoskeletal reorganization in T cells in response to fibronectin binding. These results implicated RhoG in leukocyte trafficking and the control of gene expression. Little is known about RhoG regulation, but it has been suggested that Vav proteins act as exchange factors for RhoG (27). The essential role of Vav proteins in lymphocyte development and function together with the implication of RhoG in lymphocyte signaling prompted us to study the role of RhoG in lymphocyte development and homeostasis. To this end we have generated mice in which the RhoG gene has been functionally inactivated by homologous recombination in mouse embryonic stem cells. RhoG deficiency does not have a major impact upon the development of either B or T cells. However, RhoG-deficient lymphocytes show a modestly enhanced response to antigen challenge and respond better to in vitro stimulation than their wild-type counterparts.

MATERIALS AND METHODS

RhoG gene targeting. Murine *rhog* genomic clones were isolated from a 129/Sv genomic λ phage library (Stratagene). The targeting vector consists of a 6.3-kb

TABLE 1. Lymphocyte populations in mice

Tissue and cell type	No. of cells (SD)[a]		
	Wild-type mice	RhoG$^{+/-}$ mice	RhoG$^{-/-}$ mice
Bone marrow			
Fractions A to C[b]	8.7×10^5 (2.7)	8.4×10^5 (2.2)	7.8×10^5 (1.7)
Fraction D	7.2×10^6 (1.5)	7.2×10^6 (1.6)	4.9×10^6 (0.8)
Fraction E	2.4×10^6 (0.5)	2.6×10^6 (0.6)	1.7×10^6 (0.3)
Fraction F	1.7×10^6 (0.3)	2.0×10^6 (0.2)	0.9×10^6 (0.2)
Thymus			
DP	1.9×10^8 (0.6)	ND	2.4×10^8 (0.6)
CD4	1.5×10^7 (0.4)	ND	1.8×10^7 (0.5)
CD8	2.9×10^6 (1.1)	ND	3.2×10^6 (1.0)
DN	1.4×10^6 (0.4)	ND	1.5×10^6 (0.4)
Spleen			
CD4$^+$	1.7×10^7 (0.1)	1.8×10^7 (0.1)	2.0×10^7 (0.4)
CD8$^+$	7.0×10^6 (1.7)	7.0×10^6 (1.2)	6.7×10^6 (1.6)
MZ	2.9×10^6 (1.0)	ND	2.4×10^6 (0.5)
IgM^{hi} IgD^{lo}	6.7×10^6 (1.3)	ND	7.4×10^6 (1.9)
IgM^{hi} IgD^{hi}	2.0×10^7 (1.1)	ND	1.3×10^7 (0.2)
IgM^{lo} IgD^{hi}	4.9×10^7 (1.1)	ND	4.1×10^7 (0.6)
Lymph node (%)			
CD4$^+$	39 (3)	48 (2)	42 (8)
CD8$^+$	7 (2)	7 (0)	6 (1)
B cells	39 (8)	26 (2)	35 (11)
Peritoneum: IgM$^+$CD5$^+$ (%)	26 (5)	26 (8)	26 (5)

[a] Values are the means (± SD) of flow cytometric analysis of 8-week-old mice. For determinantions of the number of cells in the bone marrow, T cells in the spleen, and cells in the lymph node and peritoneum corresponding to wild-type and heterozygous mutant mice, the number of mice (*n*) is 3. For RhoG homozygous mutant mice, *n is* 6; for determinations on the thymus, *n is* 10; and for B cell numbers in the spleen, *n* is 6. MZ, marginal zone B cells; ND, not done.
[b] Fractions were assessed using Hardy criteria (12).

*Sac*I genomic fragment inserted into the *Sac*I site of pSC-3Z, a plasmid bearing the origin of replication of pSC101 which is maintained at low copy number and suitable for propagating otherwise unstable mammalian DNA sequences in bacteria (30). A 0.9-kb *Kpn*I-*Xho*I fragment spanning the majority of exon 2 was removed and replaced with a 1.8-kb *Kpn*I-*Xho*I neomycin resistance cassette purified from pPNT (9, 31). The targeting vector was linearized with *Sac*I and electroporated into PC3 mouse embryonic stem cells (21). Following selection with G418, colonies were picked, expanded, and analyzed for the targeting event. For this purpose, *Bam*HI-digested DNA was analyzed by Southern blotting employing probe A (a 370-bp PCR product of the RhoG gene upstream of the 5′ arm of homology which was not part of the targeting vector). Of 700 clones screened, 5 were targeted. Positive clones were rescreened with probe A as well as with probe B (a 550-bp PCR product derived from DNA downstream of that included in the targeting vector). Correctly targeted clones were injected into blastocysts from C57BL/6 mice and these were transferred to pseudopregnant recipient mothers. The resulting chimeras were bred to obtain germ line transmission, which was confirmed by analysis of tail biopsy DNA. Expression of RhoG was analyzed by Northern blotting. Briefly, 10 μg of total RNA extracted from murine splenic cells was denatured and blotted onto a Hybond N+ nylon membrane (Amersham Pharmacia Biotech.). The blots were hybridized with a ^{32}P-labeled cDNA probe. Subsequently, the membrane was washed once under low-stringency conditions (2× standard saline citrate, 0.1% sodium dodecyl sulfate) and twice under high-stringency conditions (0.1× standard saline citrate, 0.1% sodium dodecyl sulfate) at 55°C for 20 min before exposure to X-ray film.

Staining of cells with fluorescent antibodies. Bone marrow, spleen, and lymph node cells were stained with monoclonal antibodies as previously described (13). Cells were analyzed on a FACSCalibur flow cytometer with Cellquest software (Becton-Dickinson). Dead cells were excluded on the basis of low forward light scatter and only live cells falling within the lymphocyte scatter gate were enumerated. All antibodies were purchased from BD-Pharmingen (San Diego, Calif.) except anti-immunoglobulin M (IgM)-Cy5 (Jackson Immunoresearch) and anti-IgD-phycoerythrin (Southern Biotechnology). Biotinylated antibodies were revealed with streptavidin-Quantum Red (Sigma).

Immunizations and Ig isotype-specific ELISA. Immunizations were carried out with 8-week-old mice injected intraperitoneally with either 25 μg of 2,4-dinitrophenol (DNP)–Ficoll in 100 μl of phosphate-buffered saline (PBS), 100 μg of DNP conjugated to keyhole limpet hemocyanin (KLH) in 100 μl of PBS, or 20 μg of DNP-lipopolysaccharide (LPS; Biosearch Technol.) in 200 μl of PBS. Serum-specific anti-DNP antibody levels were determined by ELISA as previously described (8). The relative units of DNP-specific antibodies are shown as optical density values. A dilution series of the serum samples was measured, and for each isotype a single dilution factor which fell in the linear range of the curve is represented for all time points. Serum Igs in naïve mice were determined by enzyme-linked immunosorbent assay (ELISA) using antibodies purchased from BD-Pharmingen and quantified by using purified mouse isotype standards (Sigma).

Lymphocyte proliferation assays. Splenic B and CD4$^+$ T cells were enriched by negative selection via anti-Thy-1 antibody for B cells and a mixture of anti-B220, anti-CD8, and anti-class II for T cells, followed by complement as previously described (13). The resulting cells were greater than 88% B220$^+$ or CD4$^+$ for B- or T-cell preparations, respectively, as assessed by flow cytometry. Lymphocytes were cultured for 48 h at an initial concentration of 10^6 cells/ml with the indicated doses of antibodies in RPMI 1640 supplemented with 10% fetal calf serum, 2 mM glutamine, 100 U of penicillin/ml, 100 μg of streptomycin/ml, and 0.05 mM 2-mercaptoethanol. Proliferation was measured by incorporation of [^{3}H]thymidine following a 16-h pulse.

Antigen receptor internalization. Splenic cells were isolated on a lympholyte gradient (Cerderlane) and stained either with biotinylated anti-kappa or anti-CD3 antibodies for 30 min on ice. Subsequently, cells were incubated at 37°C for the indicated times followed by the addition of ice-cold 0.5% bovine serum albumin (BSA) in PBS containing 0.1% sodium azide. Cells were stained with streptavidin-fluorescein isothiocyanate (FITC; Sigma) on ice and analyzed by flow cytometry.

Capping analysis. Purified splenic B cells were incubated with 1 μg of biotinylated anti-kappa per ml for 20 min on ice. Cells were washed in ice-cold PBS, and the primary antibody was cross-linked with anti-rat IgG (Pierce) at 37°C for 20 min. B-cell receptor (BCR) capping was stopped by the addition of 1 volume of 4% paraformaldehyde (PFA) in PBS; cells were stained with streptavidin-FITC and Phalloidin Texas red (Molecular Probes) and mounted to slides. Cells were considered to have clustered BCR if the staining pattern was polarized to one side of the cell. Images were recorded with a SPOT digital camera connected to an Axioplan 2 (Zeiss) microscope.

Calcium flux analysis. Purified splenic B cells were loaded for 30 min at room temperature in the dark with 3 μM Fluo-4 AM (Molecular Probes, Inc.) at a density of 6×10^6 cells/ml in 0.5% BSA–PBS. The cells were washed in indicator-free medium and then resuspended at 3×10^6 cells/ml in 0.5% BSA–PBS containing 1 mM $CaCl_2$ and 1 mM $MgCl_2$. After a further incubation of 30 min to allow complete de-esterification of intracellular Fluo-4 AM ester, the varia-

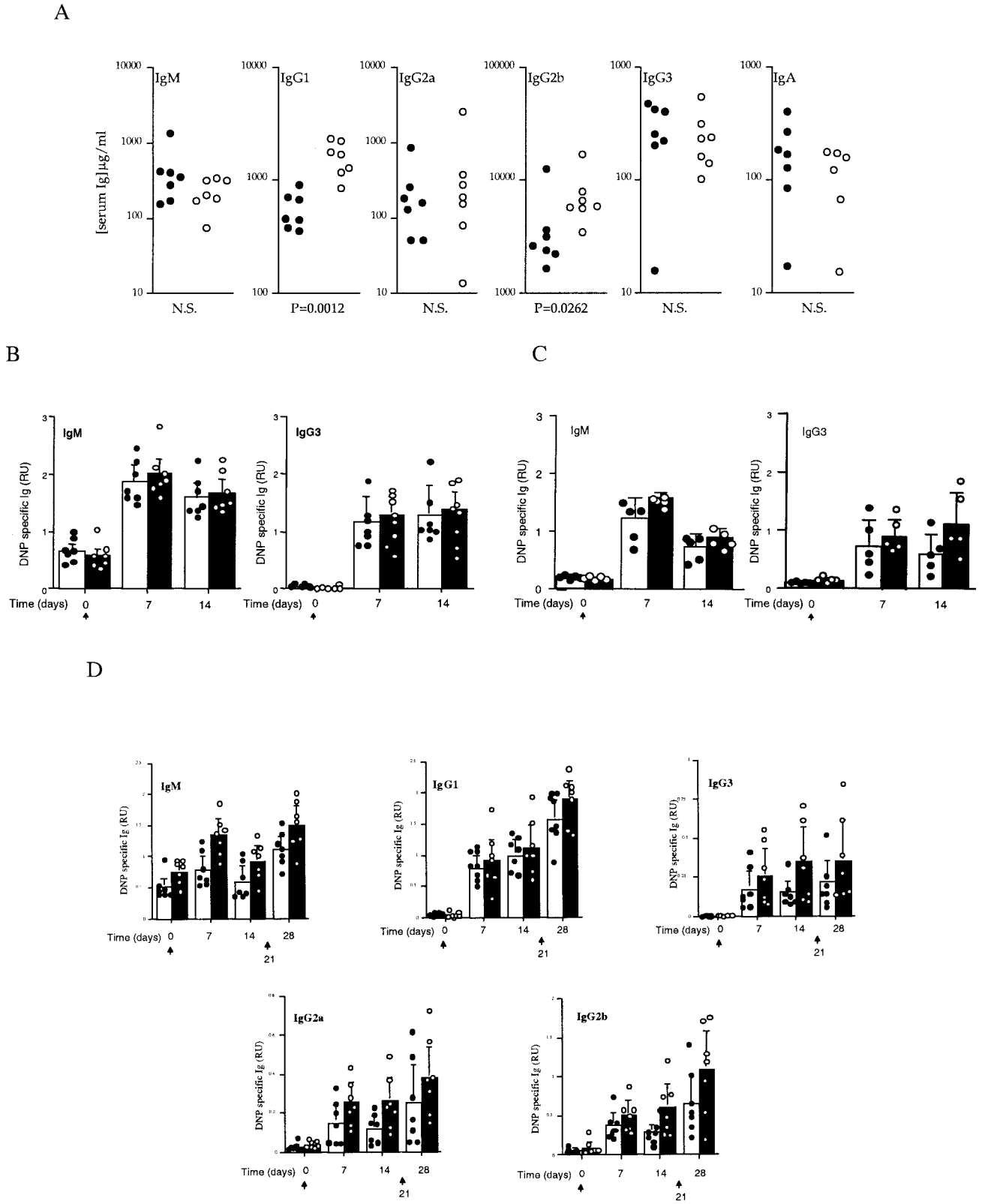

FIG. 2. Serum Ig isotypes in naïve and immunized RhoG-deficient mice. (A) Ig levels of the indicated isotypes in naïve mice. DNP-specific antibody levels from unimmunized (day 0) and DNP-Ficoll-immunized (B) and DNP-LPS-immunized (C) mice 7 and 14 days following immunization. (D) DNP-specific Ig levels of the indicated isotypes from preimmune mice and 7, 14, and 28 days post-DNP-KLH immunization. Mice were reimmunized at day 21 and bled at day 28 to assess the secondary response. In each set of graphs, individual values for control mice are represented by filled circles and for RhoG-deficient mice by open circles. Bars represent the means and standard deviations of 5 to 7 mice per group. In panels B, C, and D, the arrows indicate the days when antigen was administered. In panels B, C, and D, no significant differences were observed between wild-type and RhoG-deficient mice. NS, not significant; RU, relative units.

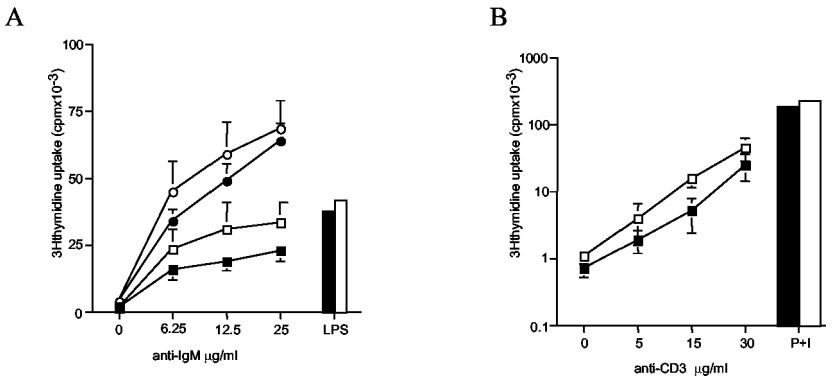

FIG. 3. Proliferative responses of RhoG-deficient lymphocytes in vitro. (A) Purified splenic B cells were cultured with the indicated doses of anti-IgM (B7.6) for 48 h with or without recombinant IL-4 or with LPS. (B) Purified splenic T cells were cultured with the indicated doses of α-CD3 or phorbol myristate acetate plus ionomycin (P+I) for 48 h. The numbers presented for each group represent counts per minute (cpm) plotted as the means and standard deviations of three individual mice analyzed in triplicate. Closed symbols, wild-type cells; open symbols, Rhog-deficient cells; circles, cells with anti-IgM and IL-4; squares, cells with anti-IgM without IL-4; bars, cells with LPS and IL-4.

tions in absorbance were measured with a Perkin-Elmer LS55 luminescence spectrometer. The intracellular calcium concentration ($[Ca^{2+}]_i$) was calculated as previously described (29).

T-helper cell differentiation assays. Splenocytes (2×10^6 cells/ml) were cultured on anti-CD3ε antibody-coated plates (10 μg of clone 2C11 per ml; Pharmingen) in the presence of exogenous cytokines or anti-cytokine antibody as indicated. Interleukin-2 (IL-2) (10 ng/ml; R&D) was added to all cultures. Th2 cell differentiation was promoted in the presence of 50 ng of IL-4 (R&D) per ml and anti-gamma interferon (IFN-γ) antibody (5 μg of clone XMG1.2/ml; Pharmingen), while Th1 differentiation was promoted by anti-IL-4 antibody at a concentration of 10 μg/ml (clone 11B11; DNAX Research Institute) and IL-12 (1 ng/ml; Genzyme, West Malling, United Kingdom). Cells were cultured for 5 days, washed, and resuspended at 2×10^6 cells/ml for 24 h in the presence of anti-CD3. Supernatants were analyzed by cytokine ELISA using the sandwich format with capture and detection antibodies purchased from Pharmingen according to the manufacturer's protocol.

T-cell stimulation. Splenocytes (2×10^6 cells/ml) were cultured on anti-CD3ε antibody-coated plates (10 μg of clone 2C11 per ml; Pharmingen) plus anti-CD28 antibody (1 μg of clone 37.51 per ml; Pharmingen) and supernatants were sampled after 24, 48 and 72 h. Supernatants were analyzed by ELISA for the presence of IL-4, IL-5, and IFN-γ (IL-4 and IL-5 were below the level of detection and are not shown).

Apoptosis. Thymocytes were γ-irradiated at the indicated doses using a cesium 137 irradiator unit, Gammacell 40 (Atomic Energy of Canada Limited). Subsequently, cells were cultured for 4 h in RPMI 1640 containing 5% fetal calf serum at 37°C, stained with Annexin V-FITC (Caltag), and analyzed by flow cytometry.

Histology and immunohistochemistry. $RhoG^{-/-}$ mice and wild-type controls were anesthetized by injection of pentobarbital (Sagatal) and perfused through the ascending aorta with cold phosphate buffer (pH 7.4) and then with freshly prepared 4% PFA in phosphate buffer (pH 7.4), and the brains were removed. After further fixation in 4% PFA overnight, the brains were then immersed in 30% sucrose (for 24 h) and then sectioned at 30 μm on a sledge microtome. Coronal sections were stained with 0.5% cresyl violet to demonstrate neural organization. Additional sections were incubated in rabbit anti-calbindin D28k serum (1) for 48 h in PBS containing 2% normal goat serum with 0.3% Triton X-100 and then incubated in biotinylated anti-rabbit IgG followed by the Vectastain ABC peroxidase reagent (Vector Laboratories, Peterborough, United Kingdom). Sections were then washed and incubated in a Vector DAB peroxidase kit to visualize the brown chromogen diaminobenzidine.

Statistical analysis. Significance of differences was evaluated with the Mann-Whitney rank sum test for the Ig measurements and with the Student *t* test for the in vitro culture assays.

RESULTS

Generation of RhoG-deficient mice. To investigate the role of RhoG in lymphocyte signaling and development, we generated RhoG-deficient mice by standard gene targeting methods with mouse embryonic stem cells (Fig. 1A). We generated a mutated allele in which the majority of exon 2, which contains the entire open reading frame, was substituted with a neomycin resistance cassette. This strategy removes both the 5′ splice acceptor and 82% of the coding potential of *RhoG* and will thus result in a null allele. Individual clones carrying the mutation (Fig. 1B) were employed to generate heterozygous and homozygous *RhoG*-mutant mice (Fig. 1C). Those mice were generated at a frequency consistent with Mendelian inheritance; they appeared healthy and reproduced normally. Northern blot analysis confirmed that the mutation lead to undetectable levels of *RhoG* mRNA (Fig. 1D).

Development of B and T cells is unaltered in RhoG-deficient mice. To study the influence of RhoG deficiency on lymphocyte development and maturation, lymphocyte lineage cells from the bone marrow, thymus, spleen, lymph node, and peritoneal cavity were analyzed by flow cytometry. No significant differences were observed in the percentages or absolute numbers of the different developmental and maturation stages of B cells in the bone marrow, spleen, or lymph nodes of $RhoG^{-/-}$ mice compared with wild-type mice as revealed in Table 1. A similar picture was observed for T cells; no major differences were found in the percentages or cell numbers between wild-type and RhoG-deficient mice (Table 1). Taken together, these results suggest that RhoG is dispensable for lymphocyte development.

$RhoG^{-/-}$ mice have elevated levels of serum IgG1 and IgG2b and respond efficiently to T-cell-dependent and -independent antigens. In nonimmunized $RhoG^{-/-}$ mice, the concentrations of serum IgG1 and IgG2b were significantly increased compared to levels in control littermates, whereas IgM, IgG2a, IgG3, and IgA levels were normal (Fig. 2A). We next tested the ability of RhoG-deficient mice to respond to thymus-independent antigens. For this purpose, mice were immunized with DNP-Ficoll, a type II antigen, and the levels of IgM and IgG3 specific for the hapten were measured at days 7 and 14 following immunization. As shown in Fig. 2B, no significant differences were observed between RhoG-deficient and control mice. Similar results were observed with the levels of DNP-specific IgM and IgG3 when mice were immunized with DNP-LPS, a type I thymus-independent antigen (Fig. 2C). Subsequently, thymus-dependent responses were evaluated by

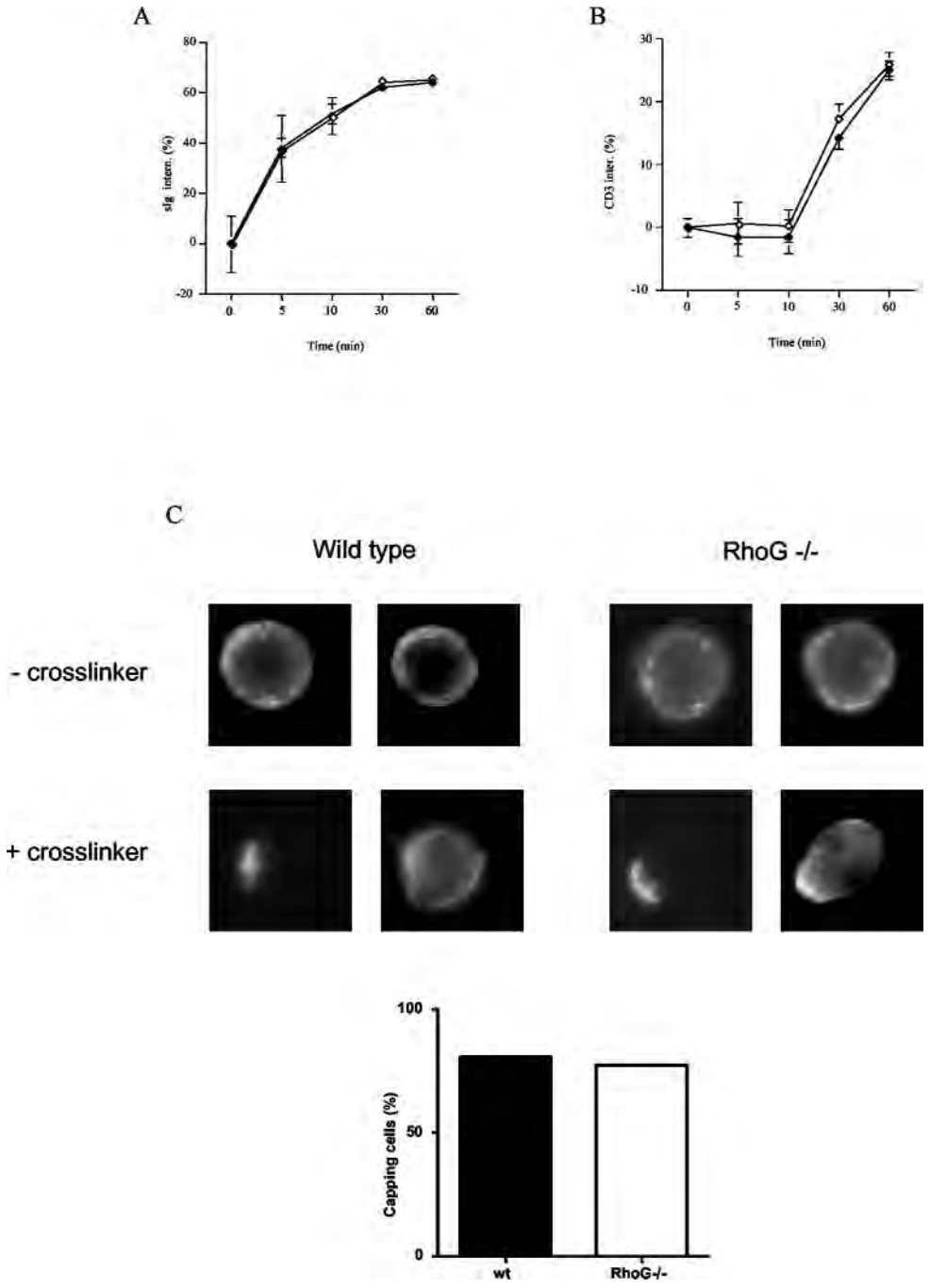

FIG. 4. Effect of RhoG on antigen receptor internalization and capping. (A and B) Splenocytes were stained with anti-kappa or anti-CD3 antibodies on ice, incubated for the indicated times at 37°C, and analyzed by a fluorescence-activated cell sorter. The numbers presented correspond to the percentage decrease of the mean fluorescence for 4 mice of each group. In each set of graphs, control cells are represented by filled symbols and RhoG-deficient cells are represented by the open symbols. (C) Purified B cells were incubated with biotinylated anti-kappa antibodies on ice, followed by cross-linking with anti-rat antibodies at 37°C for 20 min. After fixation, cells were stained with streptavidin-FITC and phalloidin Texas red to visualize cap formation (left panel) and actin polymerization (right panel). The graph shows the percentages of cells that have developed cap structures after counting 100 cells of each genotype. Inter(n), internalized.

challenging mice with DNP-KLH at days 0 and 21. Hapten-specific levels of IgM, IgG1, IgG3, IgG2a, and IgG2b were measured at days 0, 7, 14, and 28. Although no significant differences were observed between RhoG-deficient mice and their normal counterparts, there was a trend for the RhoG-deficient mice to produce higher levels of specific antibodies both for the primary and secondary responses (Fig. 2D).

RhoG-deficient lymphocytes respond to in vitro stimulation and differentiation. In order to assess the requirement for RhoG downstream of antigen receptor signaling, we first ex-

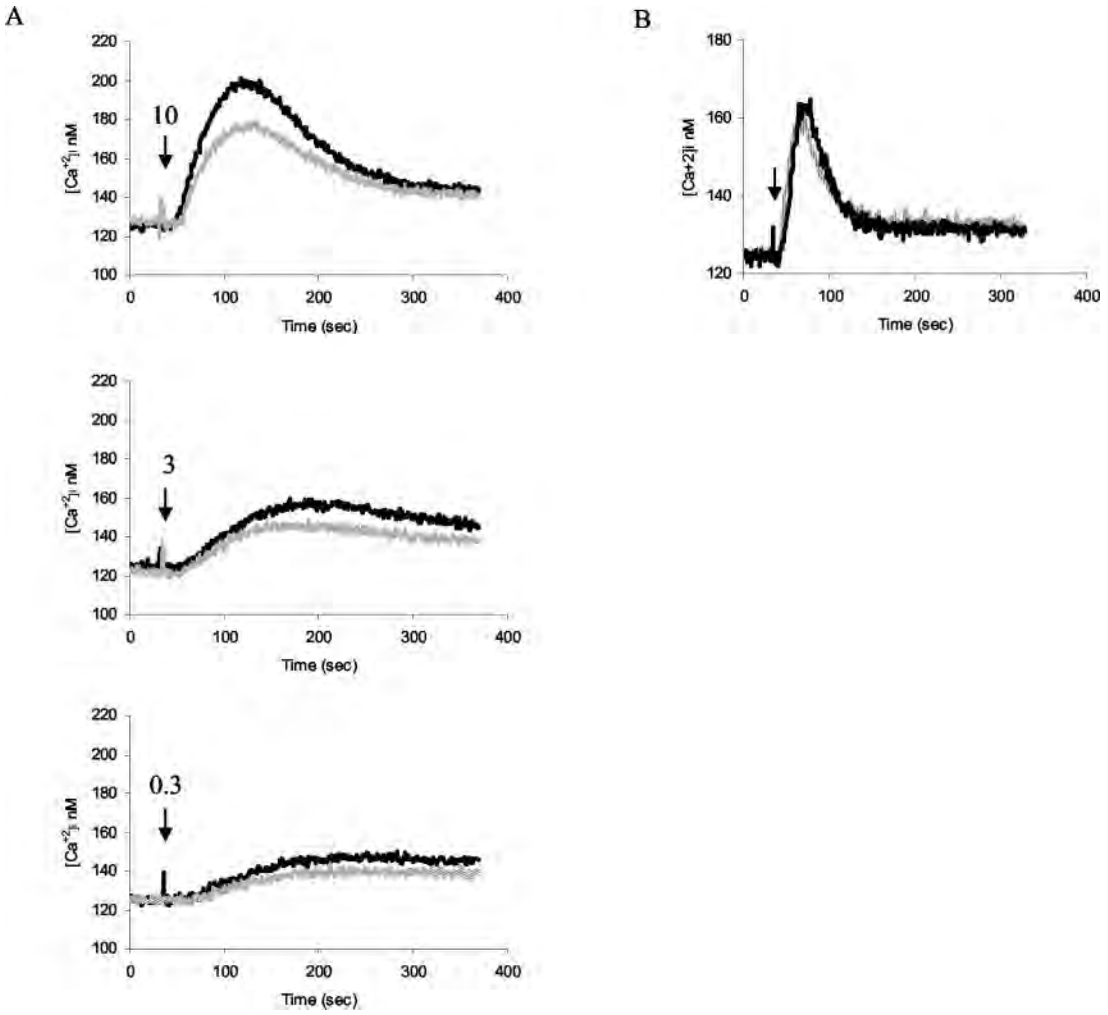

FIG. 5. Calcium response of RhoG-deficient B cells to anti-IgM is partially reduced. (A) Intracellular calcium concentration ($[Ca^{2+}]_i$) in splenic B cells after the addition of 10, 3, or 1 μg of B7.6 anti-IgM (indicated by the arrows) per ml. (B) Intracellular calcium concentration in B cells after the addition of 0.25 μg of BLC (indicated by the arrow) per ml. The black trace corresponds to wild-type cells, and the grey trace corresponds to $RhoG^{-/-}$ cells.

amined the proliferative responses of $RhoG^{-/-}$ B and T cells to antigen receptor stimulation. RhoG-deficient B cells responded slightly better to antigen receptor-triggered stimulation in the presence or absence of IL-4. By contrast, stimulation of B cells with bacterial LPS showed no difference between $RhoG^{-/-}$ and wild-type cells (Fig. 3A). A similar result was observed following activation of T cells with a monoclonal antibody to the CD3/TCR complex. $RhoG^{-/-}$ splenic T cells proliferated somewhat better than controls in response to TCR stimulation, whereas both types of cells proliferated at similar levels in response to phorbol myristate acetate in combination with ionomycin (Fig. 3B). Next, we tested the ability of $RhoG^{-/-}$ lymphocytes to internalize their antigen receptors. Both the BCR and the TCR were internalized at normal rates (Fig. 4A and B). Moreover, we assessed the ability of RhoG-deficient B cells to form a cap structure. To this end, BCR clustering was visualized after cross-linking and incubation at 37°C. In addition, polymerized actin was stained with phalloidin. In this regard, cap formation by the BCR was unaffected in the absence of RhoG (Fig. 4C, left panel). Moreover, increased actin polymerization was observed both in wild-type and RhoG-deficient B cells in the area of the cap structure (Fig. 4C, right panel). Subsequently, we studied the mobilization of intracellular calcium (Ca^{2+}) in response to BCR stimulation. We observed a modest defect in the Ca^{2+} flux elicited by BCR cross-linking of $RhoG^{-/-}$ B cells at the different doses of the agonist tested (Fig. 5A). The defect was specific to BCR cross-linking since no differences were detected in the Ca^{2+} flux between RhoG-deficient and wild-type B cells in response to the chemokine BLC (CXCL13), as shown in Fig. 4B.

To assess a role for RhoG in the regulation of gene expression, we looked at cytokine production under Th1 and Th2 cell differentiation conditions. To this end, splenic cells were cultured under conditions that promote Th1 or Th2 differentiation and the levels of IL-4, IL-5, and IFN-γ were measured. A slight decrease was observed in IL-5 production from Th2-differentiated RhoG-deficient cells compared to wild type, whereas no significant differences were observed in the production of IL-4 or IFN-γ (Fig. 6A). The ability of splenocytes to produce IFN-γ was further tested after CD3 and CD28

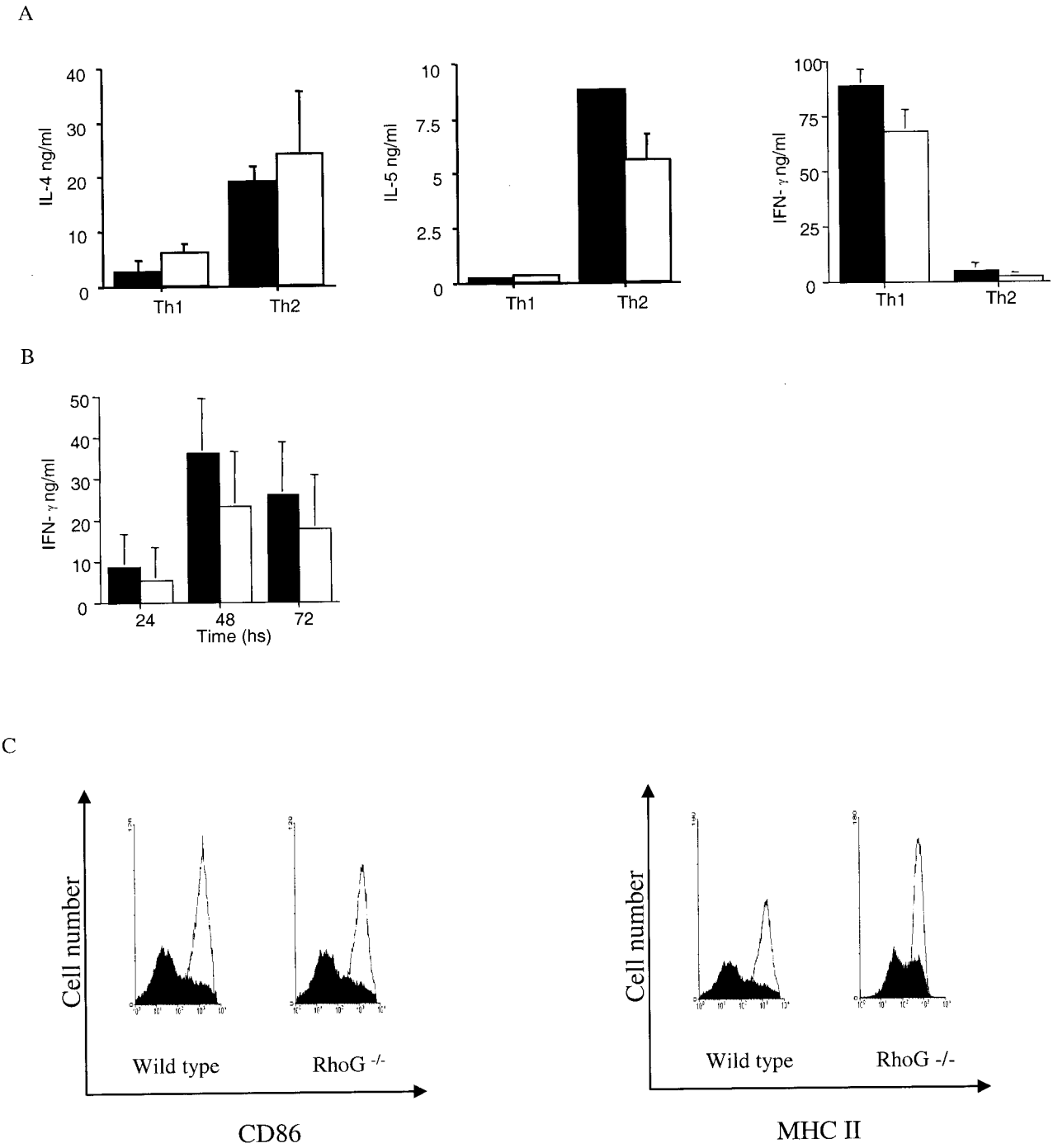

FIG. 6. Regulation of gene expression in T and B cells in the absence of RhoG. (A) Cytokine production by Th1- and Th2-differentiated cells. Splenocytes were stimulated with anti-CD3 antibodies, IL-12 and IL-2 (Th1), or IL-4 (Th2) for 5 days and then restimulated for 24 h. The supernatants were harvested and analyzed for IL-4, IL-5, and IFN-γ by ELISA. Values represent the means and standard deviations of 4 mice of each genotype. Statistical analysis of the means was assessed by the Student *t* test. For the IL-4 and IL-5 levels under Th2-differentiating conditions, $P = 0.5$ and $P = 0.03$, respectively. In the case of IFN-γ under Th1-differentiating conditions, $P = 0.06$. (B) IFN-γ production by nondifferentiated T cells. Splenocytes were treated with anti-CD3 and anti-CD28 antibodies, and the supernatants were analyzed at the indicated times for IFN-γ production. Values correspond to the means and standard deviations from 10 mice in each group. In panels A and B, control cells are represented by filled bars, and RhoG-deficient cells are represented by open bars. The *P* values for the statistical analysis of the means for IFN-γ production after 24, 48, and 72 h, comparing wild-type and RhoG-deficient cells, were 0.18, 0.5, and 0.11, respectively. (C) Induction of CD86 and MHC class II on B cells. Splenocytes were stimulated with 10 μg of α-IgM per ml for 18 h; subsequently, cells were stained with anti-B220, anti-CD86, and anti-MHC class II antibodies. The open histograms show the expression of CD86 or MHC class II antibodies on B220-positive cells after stimulation; the filled histograms correspond to the resting cells.

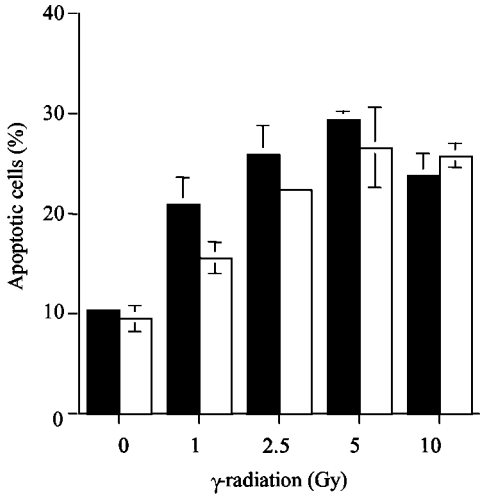

FIG. 7. Apoptosis induced by γ-irradiation. Wild-type (filled bars) and RhoG-deficient (open bars) thymocytes were treated with the indicated doses of γ-radiation, and apoptosis was measured after 4 h. Values represent the means and standard deviations of 3 mice of each genotype. Statistical analysis of the mean for wild-type and RhoG-deficient cells gave the following *P* values: 0.67, 0.13, 0.03, 0.61, and 0.41 for 0, 1, 2.5, 5, and 10 Gy, respectively.

stimulation, but again no significant difference was found between RhoG-deficient and control cells (Fig. 6B). In the case of B-cell activation, we looked at the induction of CD86 and major histocompatibility complex (MHC) class II following anti-IgM stimulation; similar results were observed in wild-type and RhoG-deficient cells (Fig. 6C).

RhoG$^{-/-}$ thymocytes undergo apoptosis in response to γ-irradiation. The rate of apoptosis induced by γ-irradiation was determined in RhoG$^{-/-}$ thymocytes. For this purpose, thymocytes were exposed to different doses of irradiation, and apoptosis was measured after 4 h. As shown in Fig. 7, a minimal decrease in the levels of apoptosis was observed in RhoG-deficient thymocytes in comparison to wild-type thymocytes.

Neural organization of RhoG-deficient mice. The neural organization of the adult RhoG$^{-/-}$ mice brain was examined and compared to that of wild-type controls. There were no obvious structural abnormalities in the adult brain. Cresyl violet-stained coronal sections at the level of the basal ganglia, hippocampus (Fig. 8A to D), and cerebellum (Fig. 8E and F) showed no organizational differences between RhoG$^{-/-}$ mice and wild-type controls. Numbers and laminar and layer patterns of neurones did not obviously differ between RhoG$^{-/-}$ mice and wild-type controls, and all the expected neuronal types (e.g., Purkinje cells in the cerebellum, pyramidal cells in the cerebral cortex, and hippocampus and granule cells in cerebellum and hippocampus) were present (Fig. 8A, B, E, and F). Use of an anti-calbindin D28k antiserum revealed the expected calbindin D28k-positive neurons in the cerebral cortex, hippocampus, and cerebellum with no obvious differences between RhoG$^{-/-}$ and wild-type mice (Fig. 8C and D).

DISCUSSION

The present study describes the immunological aspects of the phenotype of RhoG-deficient mice. We found that the absence of RhoG did not dramatically affect either B- or T-cell development. Functionally, B1 cells and marginal zone B cells seem to be normal, as the levels of serum IgM and IgG3 in naïve mice were not affected in the absence of RhoG. Moreover, antibody responses to DNP-Ficoll or DNP-LPS were indistinguishable between RhoG-deficient and wild-type mice, which is consistent with the functional properties of these B-cell subsets. However, we found elevated levels of IgG1 and IgG2b antibodies. Taken together with the tendency of RhoG$^{-/-}$ mice to produce increased levels of antibodies towards T downward antigens, our observation suggests a mild hyperreactivity defect in the RhoG$^{-/-}$ B2 cells or T cells. In agreement with this observation, in vitro proliferation of splenic B and T lymphocytes in response to antigen receptor cross-linking was slightly elevated. From a mechanistic perspective, it is not clear how these cells develop this phenotype, as they showed slightly reduced Ca^{2+} flux in response to antigen receptor stimulation, and no changes were observed in the level of expression or internalization of the antigen receptors. In addition, BCR-induced capping formation and actin polymerization were not affected in the absence of RhoG.

It has been suggested that Rac2 is involved in T-helper cell development (17). Dominant-negative Rac2-inhibited IFN-γ production in murine T cells and T cells from Rac2$^{-/-}$ mice produce decreased levels of IFN-γ under Th1-differentiating conditions in vitro. Our previous observations that constitutively active RhoG potentiated transcription from an IFN-γ promoter reporter (33), taken together with our observation of enhanced levels of serum IgG1, prompted us to study the differentiation of RhoG-deficient T cells into Th1 and Th2 subsets. However, we did not observe profound differences in the production of Th1 or Th2 cytokines. Thus, it may be concluded that RhoG does not play a role in Th differentiation or, alternatively, that RhoG function is redundant and compensated by other proteins, possibly Rac2. Considering that RhoG can potentiate NFAT activation in vitro, it is conceivable that RhoG regulates the inhibitory form(s) of NFAT to some extent. Interestingly, deficiency of NFATp or NFAT-4 in mice gives rise to modest inhibitory defects in B and T cells, but hyperresponsiveness of B and T cells and extremely high levels of Th2 cytokines and IgG1 antibodies were observed in double-knockout mice (24). The effect of RhoG deficiency on thymocyte apoptosis was evaluated. We found a minimal defect in apoptosis induced by γ-irradiation in vitro in RhoG-deficient thymocytes. However, we do not have any evidence of its physiological significance in vivo.

In addition to being expressed in lymphocytes, RhoG is expressed in the central nervous system, in particular, in the hippocampus and cerebellum (22). This fact is of particular interest as mice deficient in Trio, an exchange factor for RhoG (3), display aberrant organization in several regions within the brain, including hippocampus formation (20). Our data show no obvious changes in hippocampal organization or cerebellum morphology in the absence of RhoG.

The experiments presented in this paper show a mild defect in the immune system of RhoG-deficient mice characterized by a trend of hyperresponsiveness of B and T lymphocytes to antigen receptor engagement. Our previous study with mutant forms of RhoG and a mutant form of a RhoG effector as a dominant-negative inhibitor might have predicted a stronger

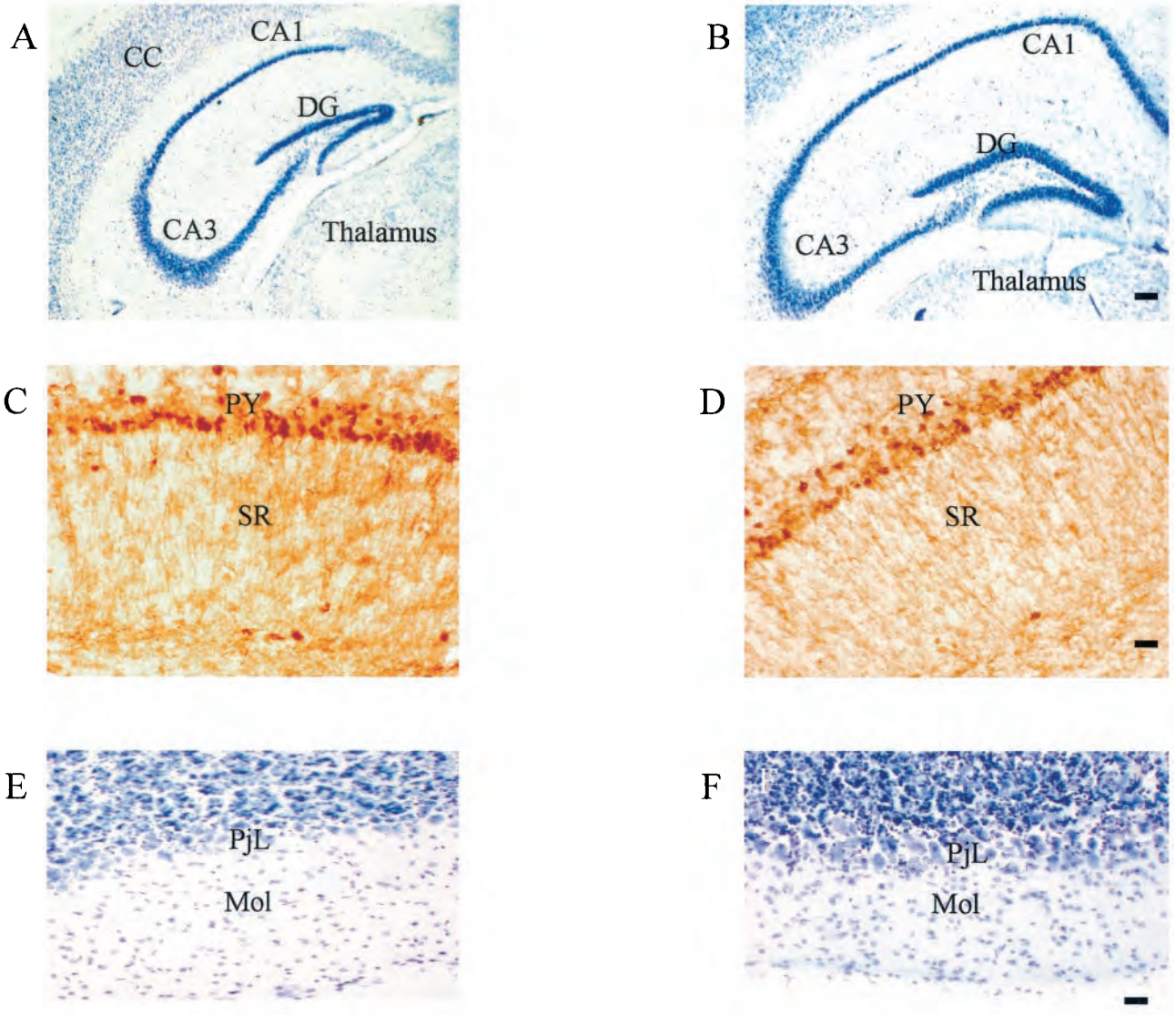

FIG. 8. Comparison of the neural organization in wild-type normal (A, C, and E) and RhoG$^{-/-}$ (B, D, and F) mice. (A and B) Coronal sections show cresyl violet staining of the hippocampus with normal hippocampal organization in both normal wild-type and RhoG$^{-/-}$ mice. (C and D) Hippocampal CA1 area visualized with an antibody raised against calbindin D28K. Note the strongly stained calbindin-positive pyramidal cells and processes in both wild-type and RhoG$^{-/-}$ mice. (E and F) Coronal sections of the cerebellum stained with cresyl violet. There were no obvious morphological differences in the cerebellum between wild-type and RhoG$^{-/-}$ mice and all other brain regions examined. Abbreviations: CC, cerebral cortex; CA1 and CA3, regions of the hippocampus; DG, dentate gyrus; PY, pyramidal cell layer of CA1; SR, stratum oriens; PjL, Purkinje cell layer; Mol, molecular layer. Scale bars: for panels A and B, 100 μm; for panels C to F, 40 μm.

phenotype (33). However, while our RhoG effector mutant is thought not to inhibit Rac and Cdc42 (35), it is relatively newly discovered and may affect other pathways yet to be identified. It is also important to point out that studies with activated and dominant-negative GTPases do not always predict loss-of-function phenotypes. Thus, dominant-mutant Rac1 has been shown to regulate planar cell polarity and ommatidial orientation in the *Drosophila* eye, while combined loss of Rac1, Rac2, and Mtl had no effect on this process (14). In this context it is worth noting that dominant-active RhoG has been found to have a different subcellular localization from wild-type RhoG (23). It is also highly possible that other small GTPases compensate for the lack of RhoG. The most likely candidates are members of the Rac family and possibly Cdc42, as these proteins are the closest to RhoG in terms of structure. Analysis of mice deficient in combinations of these proteins may elucidate the role of RhoG in lymphocyte biology.

ACKNOWLEDGMENTS

We thank C. Fernandez, M. George, and the animal facility staff for technical assistance, Eurof Walters for help with statistical analysis, and Klaus Okkenhaug for critical reading of the text.

This work was supported by a Biotechnology and Biological Sciences Research Council Competitive Strategic Grant and by grants from the Association for International Cancer Research, Leukemia Research Fund, and Cancer Research Campaign to M.T.

REFERENCES

1. **Augood, S. J., H. J. Waldvogel, M. C. Munkle, R. L. M. Faull, and P. C. Emson.** 1999. Localization of calcium-binding proteins and GABA trans-

porter (GAT-1) messenger RNA in the human subthalamic nucleus. Neuroscience **88:**521–534.
2. **Bishop, A. B., and A. Hall.** 2000. Rho GTPases and their effector proteins. Biochem. J. **348:**241–255.
3. **Blangy, A., E. Vignal, S. Schmidt, A. Debant, C. Gauthier-Rouviere, and P. Fort.** 2000. Trio GEF1 controls Rac and Cdc42-dependent cell structures through direct activation of RhoG. J. Cell Sci. **113:**729–739.
4. **Chen, F., L. Ma, M. C. Parrini, X. Mao, M. Lopez, C. Wu, P. W. Marks, L. Davidson, D. J. Kwiatkowski, T. Kirchhausen, S. H. Orkin, F. S. Rosen, B. J. Mayer, M. W. Kirschner, and F. W. Alt.** 2000. Cdc42 is required for PIP2-induced actin polymerization and early development but not for cell viability. Curr. Biol. **10:**758–765.
5. **Corre, I., M. Gomez, S. Vielkind, and D. A. Cantrell.** 2001. Analysis of thymocyte development reveals that the GTPase RhoA is a positive regulator of T cell receptor responses in vivo. J. Exp. Med. **194:**903–913.
6. **Costello, P. S., S. C. Cleverley, R. Galandrini, S. W. Henning, and D. A. Cantrell.** 2000. The GTPase Rho controls a p53-dependent survival checkpoint during thymopoiesis. J. Exp. Med. **192:**77–85.
7. **Croker, B. A., D. M. Tarlinton, L. A. Cluse, A. J. Tuxen, A. Light, F. C. Yang, D. A. Williams, and A. W. Roberts.** 2002. The Rac2 guanosine triphosphatase regulates B lymphocyte antigen receptor responses and chemotaxis and is required for establishment of B-1a and marginal zone B lymphocytes. J. Immunol. **168:**3376–3386.
8. **Doody, G. M., S. E. Bell, E. Vigorito, E. Clayton, S. McAdam, C. Fernandez, I. J. Lee, and M. Turner.** 2001. Signal transduction through Vav-2 participates in humoral immune responses and B cell maturation. Nat. Immunol. **2:**542–547.
9. **Feig, L. A.** 1999. Tools of the trade: use of dominant-inhibitory mutants of Ras-family GTPases. Nat. Cell Biol. **1:**E25–E27.
10. **Galandrini, R., S. W. Henning, and D. A. Cantrell.** 1997. Different functions of the GTPase Rho in prothymocytes and late pre-T cells. Immunity **7:**163–174.
11. **Gauthier-Rouvire, C., E. Vignal, M. Meriane, P. Roux, P. Montcourier, and P. Fort.** 1998. RhoG GTPase controls a pathway that independently activates Rac1 and Cdc42Hs. Mol. Biol. Cell **9:**1379–1394.
12. **Gomez, M., V. Tybulewicz, and D. A. Cantrell.** 2000. Control of pre-T cell proliferation and differentiation by the GTPase Rac-1. Nat. Immunol. **1:**348–352.
13. **Gulbranson-Judge, A., V. L. Tybulewicz, A. E. Walters, K. M. Toellner, I. C. MacLennan, and M. Turner.** 1999. Defective immunoglobulin class switching in Vav-deficient mice is attributable to compromised T cell help. Eur. J. Immunol. **29:**477–487.
14. **Hakeda-Suzuki, S., J. Ng, J. Tzu, G. Dietzl, Y. Sun, M. Harms, T. Nardine, L. Q. Luo, and B. J. Dickson.** 2002. Rac function and regulation during *Drosophila* development. Nature **416:**438–442.
15. **Henning, S. W., and D. A. Cantrell.** 1998. GTPases in antigen receptor signalling. Curr. Opin. Immunol. **10:**322–329.
16. **Henning, S. W., R. Galandrini, A. Hall, and D. A. Cantrell.** 1997. The GTPase Rho has a critical regulatory role in thymus development. EMBO J. **16:**2397–2407.
17. **Li, B., H. Yu, W. Zheng, R. Voll, S. Na, A. W. Roberts, D. A. Williams, R. J. Davis, S. Ghosh, and R. A. Flavell.** 2000. Role of the guanosine triphosphatase Rac2 in T helper 1 cell differentiation. Science **288:**2219–2222.
18. **Lores, P., L. Morin, R. Luna, and G. Gacon.** 1997. Enhanced apoptosis in the thymus of transgenic mice expressing constitutively activated forms of human Rac2 GTPase. Oncogene **15:**601–605.
19. **Na, S., B. Li, I. S. Grewal, H. Enslen, R. J. Davis, J. H. Hanke, and R. A. Flavell.** 1999. Expression of activated CDC42 induces T cell apoptosis in thymus and peripheral lymph organs via different pathways. Oncogene **18:**7966–7974.
20. **O'Brien, S. P., K. Seipel, Q. G. Medley, R. Bronson, R. Segal, and M. Streuli.** 2000. Skeletal muscle deformity and neuronal disorder in Trio exchange factor-deficient mouse embryos. Proc. Natl. Acad. Sci. USA **97:**12074–12078.
21. **O'Gorman, S., N. A. Dagenais, M. Qian, and Y. Marchuk.** 1997. Protamine-Cre recombinase transgenes efficiently recombine target sequences in the male germ line of mice, but not in embryonic stem cells. Proc. Natl. Acad. Sci. USA **94:**14602–14607.
22. **O'Kane, E. M., T. W. Stone, and B. J. Morris.** 2003. Distribution of Rho family GTPases in the adult rat hippocampus and cerebellum. Mol. Brain Res. **114:**1–8.
23. **Prieto-Sanchez, R. M., and X. R. Bustelo.** 2003. Structural basis for the signaling specificity of RhoG and Rac1 GTPases. J. Biol. Chem. **278:**37916–37925.
24. **Ranger, A. M., M. J. Grusby, M. R. Hodge, E. M. Gravallese, F. C. de la Brousse, T. Hoey, C. Mickanin, H. S. Baldwin, and L. H. Glimcher.** 1998. The transcription factor NF-ATc is essential for cardiac valve formation. Nature **392:**186–190.
25. **Roberts, A. W., C. Kim, L. Zhen, J. B. Lowe, R. Kapur, B. Petryniak, A. Spaetti, J. D. Pollock, J. B. Borneo, G. B. Bradford, S. J. Atkinson, M. C. Dinauer, and D. A. Williams.** 1999. Deficiency of the hematopoietic cell-specific Rho family GTPase Rac2 is characterized by abnormalities in neutrophil function and host defense. Immunity **10:**183–196.
26. **Roux, P., C. Gauthier-Rouvire, S. Doucet-Brutin, and P. Fort.** 1997. The small GTPases Cdc42Hs, Rac1 and RhoG delineate Raf-independent pathways that cooperate to transform NIH 3T3 cells. Curr. Biol. **7:**629–637.
27. **Schuebel, K. E., N. Movilla, J. L. Rosa, and X. R. Bustelo.** 1998. Phosphorylation-dependent and constitutive activation of Rho proteins by wild-type and oncogenic Vav-2. EMBO J. **17:**6608–6621.
28. **Sugihara, K., N. Nakatsuji, K. Nakamura, K. Nakao, R. Hashimoto, H. Otani, H. Sakagami, H. Kondo, S. Nozawa, A. Aiba, and M. Katsuki.** 1998. Rac1 is required for the formation of three germ layers during gastrulation. Oncogene **17:**3427–3433.
29. **Thomas, D., S. C. Tovey, T. J. Collins, M. D. Bootman, M. J. Berridge, and P. Lipp.** 2000. A comparison of fluorescent Ca2+ indicator properties and their use in measuring elementary and global Ca2+ signals. Cell Calcium **28:**213–223.
30. **Turner, M., P. J. Mee, P. S. Costello, O. Williams, A. A. Price, L. P. Duddy, M. T. Furlong, R. L. Geahlen, and V. L. Tybulewicz.** 1995. Perinatal lethality and blocked B-cell development in mice lacking the tyrosine kinase Syk. Nature **378:**298–302.
31. **Tybulewicz, V. L. J., C. E. Crawford, P. K. Jackson, R. T. Bronson, and R. C. Mulligan.** 1991. Neonatal lethality and lymphopenia in mice with a homozygous disruption of the c-abl proto-oncogene. Cell **65:**1153–1163.
32. **Van Aelst, L., and C. D'Souza-Schorey.** 1997. Rho GTPases and signalling networks. Genes Dev. **11:**2295–2322.
33. **Vigorito, E., D. D. Billadeu, D. Savoy, S. McAdam, G. Doody, P. Fort, and M. Turner.** 2003. RhoG regulates gene expression and the actin cytoskeleton in lymphocytes. Oncogene **22:**330–342.
34. **Vincent, S., P. Jeanteur, and P. Fort.** 1992. Growth-regulated expression of *rho*G, a new member of the *ras* homolog gene family. Mol. Cell. Biol. **12:**3138–3148.
35. **Wennerberg, K., S. M. Ellerbroek, R. Y. Liu, A. E. Karnoub, K. Burridge, and C. J. Der.** 2002. RhoG signals in parallel with Rac1 and Cdc42. J. Biol. Chem. **277:**47810–47817.
36. **Yang, F. C., R. Kapur, A. J. King, W. Tao, C. Kim, J. Borneo, R. Breese, M. Marshall, M. C. Dinauer, and D. A. Williams.** 2000. Rac2 stimulates Akt activation affecting BAD/Bcl-XL expression while mediating survival and actin function in primary mast cells. Immunity **12:**557–568.